Picosecond laser ranging at wavelengths up to 2.4 μm using an InAs avalanche photodiode

Silvia Butera, Peter Vines, Ian Sandall, Chee Hing Tan, Gerald S Buller

Time-of-flight measurements using pulsed laser illumination in the wavelength region between 1.3 μm to 2.37 μm have been demonstrated with an InAs avalanche photodiode (APD). InAs is photo-sensitive at wavelengths up to 3.5 μm and with predominantly electron multiplication reducing noise, InAs avalanche photodiodes have clear potential for sensitive optical measurements of fast transients in the mid-wave infrared. We describe laboratory-based demonstrations of time-of-flight ranging using InAs APDs operated at room temperature

Introduction: The mid wave infrared (MWIR) spectral range is becoming increasingly important for many applications such as gas sensing [1], thermometry [2] and LIDAR depth imaging [3, 4]. In this spectral region, semiconductor-based detectors that have been used for the detection of fast transients include InSb [5], GaSb [6] and HgCdTe [7]. These detectors have been used in linear avalanche multiplication mode for ranging and gas sensing [7]. Previously, the narrow-bandgap semiconductor materials HgCdTe [8] and InAs [9] have demonstrated predominantly electron multiplication, which led to improved detector noise performance. InAs optical detectors have potential for room temperature operation, and growth and processing techniques are typically more routinely available than alternative narrow bandgap material systems. This paper describes the use of InAs in elementary LIDAR configuration where the room temperature device was used in a fast response regime.

InAs is a narrow bandgap semiconductor with a band-gap of 0.36 eV at room temperature that allows photodetection at wavelengths of up to 3.5 μm. In avalanche photodiode operation, impact ionisation in InAs is predominantly due to electrons [9, 10], meaning that InAs APDs have potential as low-noise, high bandwidth detectors. InAs has demonstrated high gain at low reverse bias allowing the potential of routine operation in arrayed detector geometries. In applications such as LIDAR, InAs APDs offer fast timing which can result in MWIR ranging with excellent surface-to-surface resolution. This is mainly due to the impact ionisation properties of the electron-multiplying APD, where the avalanche current can build up in a single transit in the multiplication region.

In this paper, for the first time, laboratory-based time-of-flight experiments, over ranges of around 0.5 metre stand-off distance, were performed with an InAs mesa APD. The APD was used in linear multiplication mode, demonstrating time-of-flight measurements at wavelengths up to 2.37 μm. Moving a retro-reflective target to different positions and recording the corresponding time of flight gave high precision range measurements.

Experiment N-i-p mesa photodiodes were grown by the National Centre for III-V Technologies at the University of Sheffield by molecular beam epitaxy (MBE). A constant doping concentration of 1×10^{18} cm^{-3} was used for the p and n layers. The layer's thicknesses were 2 μm for the n-region, 4 μm for the i-region and 1.5 μm for the p-region. After growth, the wafer was processed to form mesa structures. Trials have shown that the best recipe for mesa etching was in 1:1:1 H_3PO_4: H_2O_2: H_2O solution followed by 30 s in a 1:8:80 H_2SO_4: H_2O_2: H_2O solution [11]. Once the InAs mesas were formed, they were passivated with the photoresist SU8. The devices were processed with a mask set that combined the SU8 with SiN (because of its good adhesion with the top metal contact) under the external metal bondpad in order to produce a packaged mesa InAs APD. A 100 μm diameter n-i-p structure was used at room temperature throughout this study.

Figure 1 shows a schematic of the experimental set up used for these time-of-flight ranging experiments. The 40 MHz pulsed supercontinuum laser (NKT Photonics SuperK Extreme EXW-6) was directed through a 50:50 beam splitter to the centre of a movable retroreflective mirror. The beam returning from the retroreflector was then reflected by the beam splitter and focussed onto the detector using a ×5 magnification microscope objective lens, L2. To monitor the laser illumination on the detector prior to the actual measurement, a white light source and InGaAs-based camera were used to image the device plane in order to align the laser spot on the detector. When light was detected, the detector provided an output pulse due to the photocurrent generated in the device. A high pass filter was used to remove the DC dark current component. A picosecond timing card (Becker and Hickl SPC 600) was used to record the pulse arrival time relative to the laser reference signal.

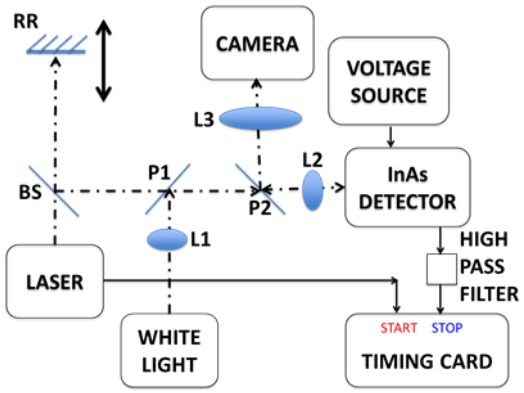

Fig 1 *Experimental LIDAR set up. Solid lines denote electrical connections, while dashed lines free space optical paths. L1, L2 and L3 represent optical lenses, P1 and P2 represent 90:10 pellicle beam splitters, BS the 50:50 beam splitter and RR the retroreflector.*

During the experiment the retroreflector was moved along the optical axis over a distance of about 0.5 m at 5 cm increments to delay the returning optical signal. The retroreflector scan was performed for different wavelengths in the infrared spectral range by tuning the supercontinuum laser from 1.3 to 2.37 μm. The sample was reverse biased up to a maximum of 6.5 V.

To estimate the device jitter, we measure the time difference between the detector output (the STOP signal pulse) with respect to a reference signal (the START signal pulse) given by the laser pulse. By sampling many laser pulses, a timing histogram of the measured START-STOP time differences was constructed, which gave the temporal response of the overall detection system. This histogram was obtained at various retro-reflector positions to ascertain the time of return for each position. This time position was ascertained by finding the centroid of each peak, where the centroid is calculated as a weighted sum: each histogram bin arrival time t_k was weighted by the number of photons within the bin. The histogram acquisition times were varied between 5 and 20 s to achieve a measurement with approximately 10^6 detection events for each retroreflector position. A typical timing histogram using this detector approach is shown in Fig 2, corresponding to the time response of the system when illuminated by the laser at 2.1 μm wavelength and reverse biased at 2.5 V.

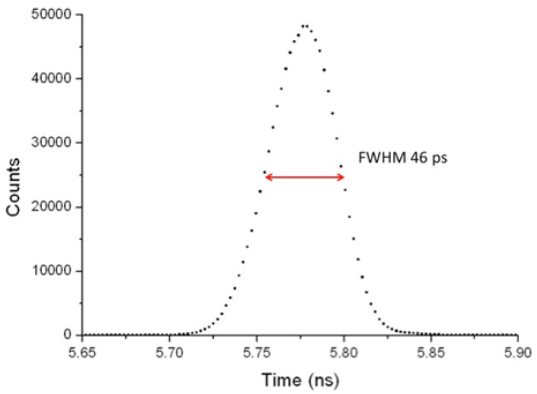

Fig. 2 *Example of a timing histogram when the APD is illuminated by the laser at 2.1 μm wavelength.*

As shown in Figure 2, the shape of the system temporal response was a near Gaussian centred with a full width at half maximum (FWHM) of 46 ps. This fast timing jitter is partly due to the relatively high laser power (the average laser power at the cryostat window was 30 µW) used and thus the large number of photons incident on the detector within an optical pulse allowing a low multiplication to be used to amplify the signal. Nevertheless, since InAs is a predominantly electron-multiplying APD we expect that at high multiplication values the impact ionisation process will occur mostly in only one transit time of the multiplication region, resulting in significantly lower jitter than conventional high gain APDs and SPADs [12].

As a demonstration of the depth resolution of the InAs avalanche photodiode LIDAR system, the detector output pulse arrival time was plotted as a function of the retroreflector position, an example of which is shown in Figure 4 at a wavelength of 2.3 µm. During the ranging experiment, the retroreflector position was scanned for a range of wavelengths between 1.3 µm and 2.3 µm. As illustrated in Fig. 3, the time-of-flight is shown against corner-cube movement (i.e. half the round-trip), hence the gradient will be equal to half the speed of light. The graph gives an estimation of the speed of light and error as $2.991 \pm 0.045 \times 10^8$ ms^{-1}.

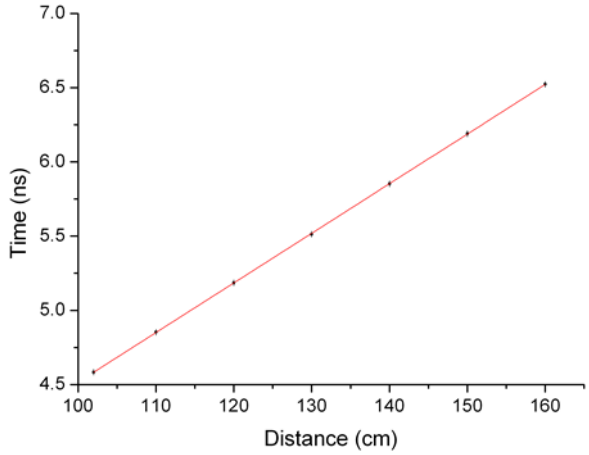

Fig 3 *Variation in time of APD output pulse arrival as a function of retroreflector position using $\lambda = 2.3$ µm radiation.*

Conclusions We have demonstrated picosecond resolution LIDAR measurements using an InAs avalanche photodiode. Using a picosecond pulsed laser and picosecond timing hardware more commonly used in time-correlated single photon counting, the InAs APD was triggered on the rising edge, achieving a jitter of 46 ps. We demonstrated this jitter performance at wavelengths up to 2.37 µm, with this spectral range being only limited by the emission spectrum of the tunable supercontinuum laser source used in these experiments.

Using our packaged n-i-p InAs devices operating at room temperature and at low gain, we show that a time of flight technique can be used at wavelengths up to 2.37 µm. InAs APDs offer the potential for low timing jitter, high accuracy MWIR ranging, even at high multiplication. This is mainly due to the intrinsic properties of the electron APD, where the avalanche builds up in a single transit in the multiplication region. Furthermore, taking measurements of the output pulse arrival time as a function of the retroreflector position, the gradient fitted the speed of light within the experimental error.

References

1. Adler F., Masłowski P., Foltynowicz A., Cossel K.C., Briles T.C., Hartl I., and Ye J., "Mid-infrared Fourier transform spectroscopy with a broadband frequency comb," Opt. Express, 2010, **18**, pp. 21861-21872
2. Jadin M.S., and Taib S., "Recent progress in diagnosing the reliability of electrical equipment by using infrared thermography," Infrared Physics & Technology, 2012, **55**, 236-245
3. McCarthy A., Krichel N.J., Gemmell N.R., Ren X., Tanner M.G., Dorenbos S.N., Zwiller V., Hadfield R.H., and Buller G.S., "Kilometer-range, high resolution depth imaging via 1560 nm wavelength single-photon detection," Opt. Express, 2013, **21**, 8904-8915
4. de Borniol E., Rothman J., Guellec F., Vojetta G., Destéfanis G., and Pacaud O., "Active three-dimensional and thermal imaging with a 30-µm pitch 320×256 HgCdTe avalanche photodiode focal plane array," Op. Eng., 2012, **51**, 061305 1-6
5. Degtiarev, E.V., Geiger, A.R. and Richmond, R.D., "Compact dual wavelength 3.30-3.47µm DIAL lidar", Proc. SPIE, 2000, **4036**, pp 229-235,.
6. Diagne M., Greszik M., Duerr E., Zayhowski J., Manfra M., Bailey R., Donnelly J., and Turner G., "Integrated array of 2 µm antimonide-based single-photon counting devices," Opt. Express, 2011, **19**, 4210-4216
7. Lambert-Girard S., Allard M., Piché M., and Babin F., "A differential optical absorption spectroscopy lidar for mid-infrared gaseous measurements,", Appl. Opt., 2015, **54**, pp. 1647-1656
8. Beck J., Wan C., Kinch M., Robinson J., Mitra P., Scritchfield R., Ma. F., and Campbell J., "The HgCdTe electron avalanche photodiode," J. Electron. Mat., 2006, **35**, 1166-1173
9. Marshall A.R., David J.P., and Tan C.H., "Impact ionization in InAs electron avalanche photodiodes," IEEE Trans. Electron Dev., 2010, **57**, 2631-2638
10. Marshall A.R.J., Vines P., Ker P.J., David J.P., and Tan C.H., "Avalanche multiplication and excess noise in InAs electron avalanche photodiodes at 77 K," IEEE J. Quant. Electron., 2011, **47**, 858-864
11. Marshall A.R.J., Tan C.H., David J.P.R., Ng J.S. and Hopkinson M., "Fabrication of InAs photodiodes with reduced surface leakage current," Proc. SPIE, 2007, **6740**, pp. 67400H,.
12. Marshall A.R., Ker P.J., Krysa A., David J.P., and Tan C.H., "High speed InAs electron avalanche photodiodes overcome the conventional gain-bandwidth product limit," Opt. Express, 2011, **19**, pp 23341-23349

Silvia Butera, Peter Vines and Gerald S Buller. *(Institute of Photonics and Quantum Sciences, Heriot-Watt University, Edinburgh, EH14 4AS, UK)*

Ian Sandall and Chee Hing Tan *(Deptartment of Electronic & Electrical Engineering, University of Sheffield, Sheffield, S1 3JD, UK)*